Vol. 599: 1–18, 2018
https://doi.org/10.3354/meps12646

MARINE ECOLOGY PROGRESS SERIES
Mar Ecol Prog Ser

Published July 12

FEATURE ARTICLE

Factors controlling the seasonal distribution of pelagic *Sargassum*

Maureen T. Brooks[1,*], Victoria J. Coles[1], Raleigh R. Hood[1], Jim F. R. Gower[2]

[1]University of Maryland Center for Environmental Science, Horn Point Laboratory, PO Box 775, Cambridge, MD 21613, USA
[2]Fisheries and Ocean Canada, Institute of Ocean Sciences, Sidney, BC V8L 4B2, Canada

ABSTRACT: Pelagic *Sargassum* (*S. fluitans* and *S. natans*) is endemic to the tropical and subtropical North Atlantic, where it provides habitat for a diverse and economically important ecosystem. Here, we investigate what controls the *Sargassum* seasonal distribution using a coupled modelling approach that integrates output from a data-assimilating 1/12° HYCOM simulation, a 1/4° coupled HYCOM–biogeochemical model, and individual-based Lagrangian *Sargassum* growth models. Passively advected, buoyant particles with no *Sargassum* physiology aggregate in the central North Atlantic Subtropical Gyre at annual time scales and do not show distributions consistent with satellite observations of *Sargassum*. However, at shorter time scales, advection alone can explain up to 60% of the following month observed distribution during some periods of the year. Connectivity between the tropical Atlantic and Sargasso Sea is largely one-way, with the Sargasso Sea acting as a 'dead end' for *Sargassum*. Adding growth, mortality and a simple formulation of reproduction through fragmentation to the passive advection of *Sargassum* particles generates distributions that match observations with 65 to 75% accuracy across all seasons. Incorporating both ocean circulation and *Sargassum* physiology appears to be key in successfully reproducing the seasonal distribution of biomass. We propose a conceptual model of the *Sargassum* seasonal cycle that incorporates new information about a population in the tropical Atlantic. Additionally, we suggest that the Gulf of Mexico and Western Tropical Atlantic are regions whose *Sargassum* populations may disproportionately influence the basin-wide biomass.

KEY WORDS: Pelagic *Sargassum* · Macroalgae · Lagrangian transport

*Corresponding author: mbrooks@umces.edu

Pelagic *Sargassum* contributes structural habitat to the surface waters of the tropical and subtropical Atlantic Ocean. *Photo: Victoria J. Coles*

INTRODUCTION

Observations of pelagic *Sargassum* date back centuries (Dickson 1894), sparking debate over its origins and life history for much of that time (Deacon 1942). The species of the brown macroalgae (Phaeophyceae) *Sargassum*, *S. fluitans* and *S. natans*, form floating aggregations or 'rafts' over much of the tropical and subtropical North Atlantic. Both species are holopelagic, having no attached benthic stage in their life cycle, and reproduce solely vegetatively by fragmentation (Butler et al. 1983, Stoner 1983).

Changes in *Sargassum* abundance from the early to the late 20th century have been suggested but

Publisher: Inter-Research · www.int-res.com

have proven difficult to verify (Parr 1939, Stoner 1983). Seasonal variability in *Sargassum* distribution and biomass coupled with seasonality in the sparse observations led to this perceived decline (Butler & Stoner 1984). More recently, *Sargassum* distribution throughout the annual cycle has been mapped via satellite (Gower & King 2011, Gower et al. 2013, Wang & Hu 2016). The remote sensing derived distributions also suggest that changes in biomass and southern range expansion have occurred in recent years (Gower et al. 2013, Wang & Hu 2016), and field observations suggest this may be influencing species and morphotype composition in the Caribbean (Schell et al. 2015). *In situ* observations confirm that *Sargassum natans* occurs off the coast of Brazil, south of the presumed range (Széchy et al. 2012, Sissini et al. 2017). Franks et al. (2016) suggest this is related to a recirculation in the tropical gyre. These range and biomass changes coincide with an increase in reports of beaching events affecting fishing and tourism from Africa to the Caribbean (Franks et al. 2011, Smetacek & Zingone 2013), which prompted the development of a satellite-based *Sargassum* early warning system for the region (Webster & Linton 2013). Understanding what environmental factors are controlling recent variability is difficult, however, without a better understanding of what is driving variability in *Sargassum* distribution on seasonal time scales.

Remote sensing algorithms for *Sargassum* exist for sensors such as the Medium Resolution Imaging Spectrometer (MERIS) and Moderate Resolution Imaging Spectroradiometer (MODIS) satellites because floating vegetation causes enhanced reflectance in the near-infrared (Gower et al. 2006, Hu et al. 2015). Satellite observations (Gower et al. 2006, Gower & King 2011) from 2002 through 2010 demonstrate a seasonal cycle in *Sargassum* distribution initiating in April when integrated basin-wide biomass is at a minimum. High abundances occur in the Gulf of Mexico in the spring and early summer, in the Gulf Stream extension region in late summer and early fall, and in the southern Sargasso Sea in the winter and early spring (Fig. 1). High abundances are also suggested (but with little direct validation) in the tropical gyre in late spring through fall. Subsequent years show the influence of the high biomass seen in the western tropics (Gower et al. 2013, Wang & Hu 2016).

Buoyant *Sargassum* is expected to passively follow surface currents and local eddy fields (Zhong et al. 2012), although there are suggestions that inertial effects acting directly on *Sargassum* rafts could cause their trajectories to differ from that of the surrounding water and influence their distribution (Beron-Vera et al. 2015). However, pelagic *Sargassum* has a minimum doubling time of 9 to 13 d, depending on species (Hanisak & Samuel 1987), which is short relative to advection time scales. Thus, *Sargassum* may not act as an entirely passive tracer, since its distribution can be influenced by growth and mortality in addition to advection. *Sargassum* primary production varies across its range (Carpenter & Cox 1974), and is generally higher in neritic waters with higher nutrient availability (Lapointe 1995). Pelagic *Sargassum* underpins a diverse ecosystem (Butler et al. 1983, Laffoley et al. 2011, Huffard et al. 2014) supporting a wide range of fish species (Hoffmayer et al. 2005) and playing a role in the migration of juvenile sea turtles (Carr & Meylan 1980, Witherington et al. 2012). Some evidence suggests that the macroalgae may even be responsive to excretion of ammonium and phosphorus from associated fish species (Lapointe et al. 2014). This raises the question of the extent to which the observed seasonal pattern is a result of passive advection of *Sargassum* around the Atlantic, versus due to growth and mortality of *Sargassum* rafts as they encounter changing environmental conditions.

In this study we use a numerical model to investigate what controls the distribution and seasonal cycle of *Sargassum* in the North Atlantic and Gulf of Mexico. Physical circulation and Lagrangian particle advection models are used to estimate the contribution of advection to the *Sargassum* seasonal distribution. This is accomplished via analysis of particle trajectories, particle densities, and regional connectivity. The influence of *Sargassum* growth and mortality is examined by adding an algal physiology model, coupled to a biogeochemical model embedded within the circulation. The simulations suggest spatial and temporal variability in *Sargassum* growth regions strongly influences basin-wide seasonal biomass patterns.

METHODS

Data description and validation

Sargassum biomass is derived from satellite imagery from the European Space Agency MERIS sensor (Rast et al. 1999). A climatology of *Sargassum* biomass is generated from monthly 1° gridded MERIS counts from 2002 to 2012, with an estimated 1400 t (wet weight) of *Sargassum* per grid per MERIS count (Gower & King 2011, Gower et al. 2013). The resulting distribution is smoothed with an adjustable-

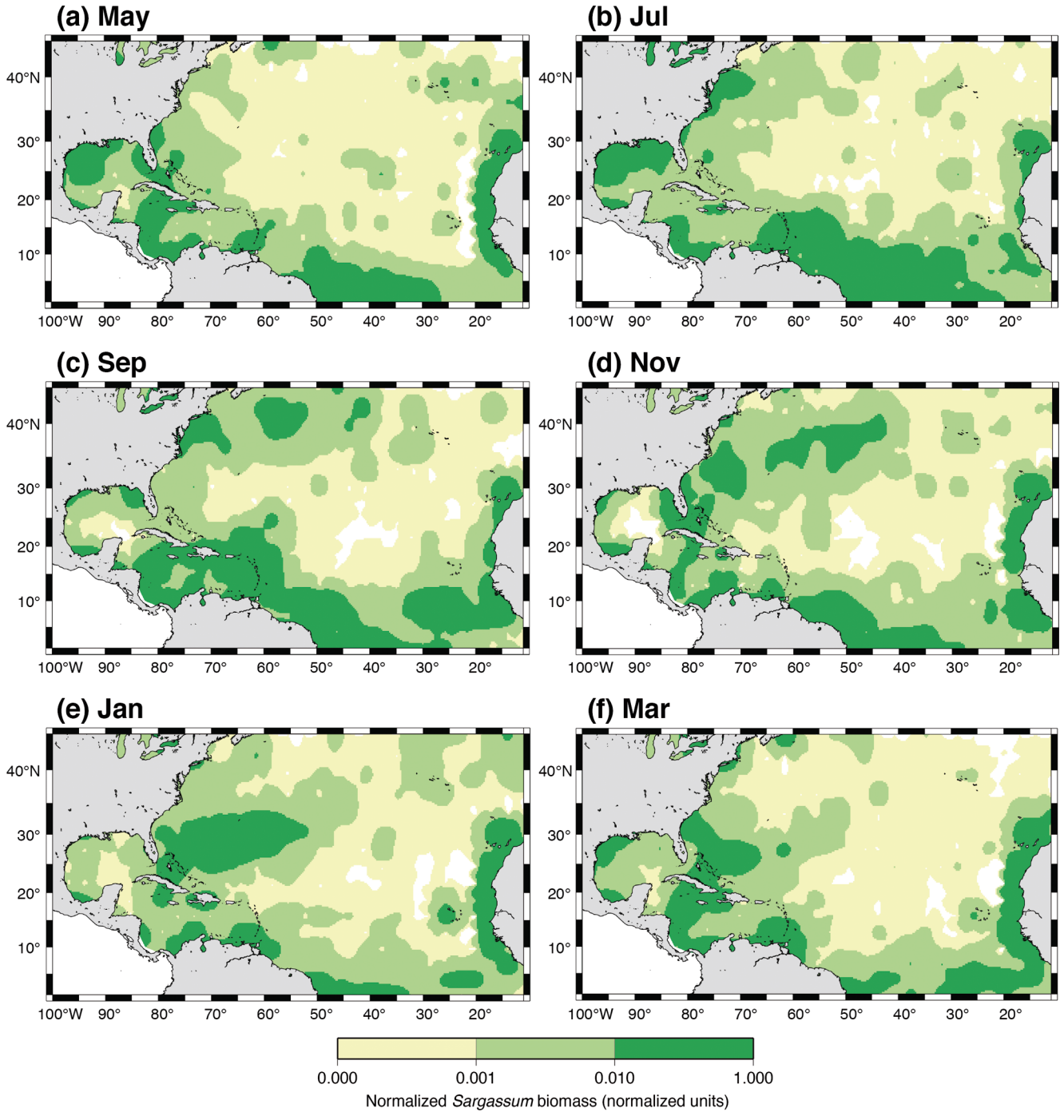

Fig. 1. Relative *Sargassum* biomass based on monthly satellite climatologies from Gower & King (2011), Gower et al. (2013). Each panel represents a different month, with the seasonal cycle initiating in the spring when integrated basin-wide biomass is at its annual minimum

tension continuous curvature spline with a tension factor of 0.25 (Fig. 1). The climatology illustrates the seasonal changes in *Sargassum* biomass in the key habitat regions of the Gulf of Mexico and Sargasso Sea, as well as potentially high *Sargassum* abundance in the tropics.

Both MERIS and MODIS observations show what appears to be a regime shift in *Sargassum* in the tropics, initiating with a high biomass event in 2011 (Gower et al. 2013, Wang & Hu 2016). However, smaller amounts of *Sargassum* have been detected in the region over the entire satellite record (Gower &

King 2011, Wang & Hu 2016). A second climatology using only the period 2002 to 2010 shows a similar overall seasonal pattern and phenology, though with reduced tropical biomass. Thus, here we use the full 2002 to 2012 climatology, which gives a robust description of the seasonality in the subtropics and also includes the signal of the modern tropical regime.

Only limited observations were available to Gower & King (2011) for algorithm validation. Anomalies such as satellite detection of Maximum Chlorophyll Index (MCI) signal in the Pacific outside of the known range of *Sargassum*, and the large biomass in the tropics where there had been few direct observations of *Sargassum* until recently (Széchy et al. 2012) motivate further validation. The Sea Education Association has performed neuston tows from 1973 to 2010 (Siuda 2011). In spring, low to no *Sargassum* is found in tows along 65° W from 20 to 40° N and higher densities are found south of 32° N and west of 65° W (Siuda 2011). This pattern is consistent with the May satellite climatology (Fig. 1), which has the lowest densities in the Sargasso Sea, with some moderate biomass to the south and west. In fall, low densities are found in tows south of 30° N along 55 to 60° W, and higher densities (0 to 3 g m^{-2}) are found between 30 and 40° N and extending towards the US East Coast from 55 to 70° W. This is broadly consistent with the September to November satellite climatologies, when moderate to high density regions of *Sargassum,* defined as having greater than 1% of maximum possible MCI signal, extend over the largest area of the Sargasso Sea. This band of high biomass stretches from 35° N to nearly 50° N, beyond the range of direct observations. Satellite detection of abundant *Sargassum* stretching north from the eastern Caribbean to near 24° N from 60 to 65° W in September is less consistent with the limited ship-based data, which suggests low *Sargassum* biomass in this location.

Within the Gulf of Mexico, higher satellite observed densities are seen in spring (March) and increase to over half the area of the Gulf in July (Fig. 1) and August (not shown). Like the Sargasso Sea, the Gulf of Mexico also experiences seasonal periods of low or undetectable *Sargassum* densities, but in January rather than May. In contrast, the Caribbean and central tropics (east of 60° W, south of 15° N) have *Sargassum* year-round. In these regions, the extent of the moderate to high densities are the largest in the late summer (September).

Physical model description

Daily output from a data-assimilating Hybrid Coordinate Ocean Model (HYCOM) simulation (Chassignet et al. 2009) is used to advect Lagrangian particles. This is an eddy-resolving (1/12° ~7 km resolution) global model run by the Naval Research Laboratory (HYCOM.org GLBa0.08 expt_ 90.9). The model has 32 hybrid vertical layers, 11 of which are fixed-depth in the upper 60 m of the water column including a 1 m thick surface layer. The high surface vertical resolution is ideal for modeling *Sargassum,* whose buoyancy begins to diminish at depths below 35 m and is fully compromised below 120 m (Johnson & Richardson 1977). Surface forcing, including wind speed, wind stress, precipitation and heat flux is from the Navy Operational Global Atmospheric Prediction System. The shortwave radiation forcing has an analytic diurnal cycle superimposed. Three-dimensional multivariate data assimilation is performed via the Navy Coupled Ocean Data Assimilation system (Cummings 2005, Cummings & Smedstad 2013).

The HYCOM particle-tracking code (Halliwell et al. 2003), based on particle advection schemes from the Miami Isopycnal Coordinate Ocean Model (Garraffo et al. 2001) is used to advect idealized *Sargassum* rafts. Daily instantaneous model velocities, interpolated to 4 h intervals using second-order Runge–Kutta, are used as input for the Lagrangian particle model, which treats particles as water parcels with respect to inertial forces. Solutions are insensitive to realistic values of diffusion (< 1% difference in pairwise particle density at 60 d time scales with added horizontal turbulence velocity variance of 4.63×10^{-6} m^2 s^{-2}). The code is modified for this study to allow specification of float buoyancy (here set to 0.1 m s^{-1} following Johnson & Richardson 1977). This is achieved by adding this rate of rise to the vertical velocity after interpolation of the velocity fields from HYCOM to the particle location. Additional modifications allow for running particles backwards in time by reversing the time step and velocities. All particles in this study are initialized in the uppermost meter to represent buoyant healthy *Sargassum* rafts. Experimental information, including particle release dates and tracking times are specified in Table 1. To mitigate the effects of interannual variability, we launch particles in a total of 8 different model years, 2 at 1/12° resolution for physics-only experiments and 6 at 1/4° resolution (Table 1). We track individual particles for 2 yr after initialization. Following best practices for particle models of bio-

logical–physical interactions we quantitatively evaluate the optimum particle number for model experiments (North et al. 2009). The number of model particles required to obtain stable statistics is determined using the fraction of unexplained variance (FUV) method described by Simons et al. (2013). Particle initializations range from 20 to 280 particles daily, randomly distributed over the domain of interest over 2 yr (Fig. 2). Particle density distribution (PDD) is calculated as the number of particles of a given age in a 2° box divided by the total number of particles released. The FUV is calculated as $1 - r^2$ of the linear correlation coefficient between the PDD at each intermediate total particle count and the final total count of particles. At 60 d (Fig. 2a) FUV does not reach the acceptable threshold of 0.05 until there are more than 30 000 particles. As particles approach a year of deployment time variability decreases and FUV is <0.025 with only 15 000 particles. Low particle number leads to variability in FUV, with a decreasing trend as particles age (Fig. 2b). At particle numbers over 50 000, FUV is within acceptable limits and shows little change with particle age. An initialization of 51 100 particles (140 d^{-1}) is used as a baseline particle number for our simulations because it is highly correlated (FUV < 0.01) with a larger doubled distribution of 280 particles d^{-1} over particle ages ranging from 30 to 360 d in the region of interest.

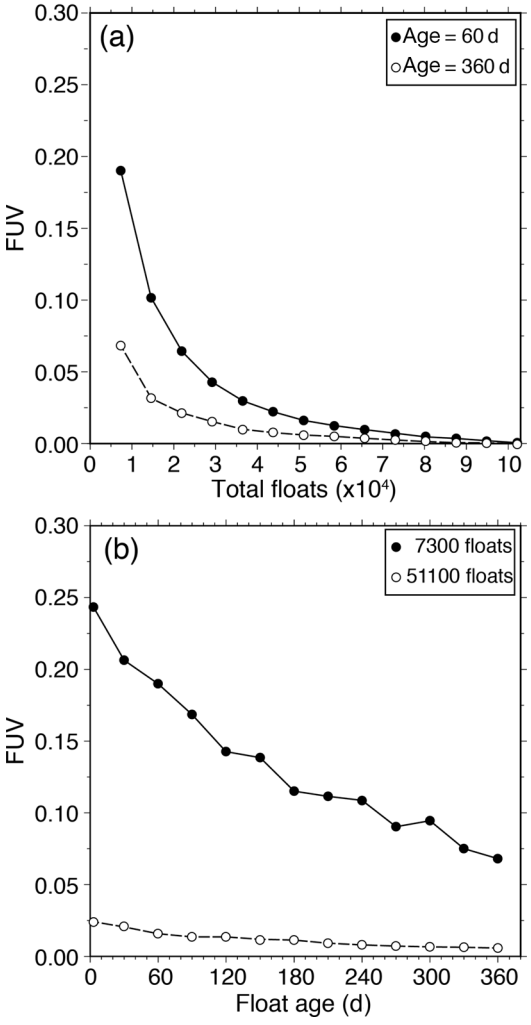

Fig. 2. Fraction of unexplained variance (FUV) (a) as particle numbers increase, and (b) as a function of particle age. Comparison is with a reference run with 102 200 particles (280 particles released d^{-1})

Biogeochemical model description

To understand the impact of processes such as light and nutrient availability on *Sargassum*, we developed a biogeochemical model. This is nested within a 1/4° HYCOM simulation with an Atlantic domain from 15° S to 62° N and 100° W to 15° E. A 6-hourly surface forcing is based on the European Centre for Medium-Range Weather Forecasts (ECMWF) reanalysis (Uppala et al. 2005) and simulations are run for years 1983 to 1988.

The biogeochemical model consists of 2 nitrogen species (NO_3, NH_4), dissolved inorganic phosphorus (DIP), 2 phytoplankton (an open-ocean phytoplankton assemblage, and a diazotroph mod-

Table 1. Lagrangian particle experiments. Experiments with multiple resolutions listed were replicated at each resolution. The 1/12° model is the global, data-assimilating HYCOM experiment 90.9 for years 2011 to 2012. The 1/4° model is the Atlantic domain model with coupled biogeochemistry developed for this study, for years 1983 to 1988

Expt	Particle	Distribution	Model resolution (°)	Tracking time
R-ISO	Isobaric	Whole domain	1/12, 1/4	Forward
R-3D	3-D	Whole domain	1/12, 1/4	Forward
R-3DB	3-D, buoyant	Whole domain	1/12, 1/4	Forward
C-ISO	Isobaric	Climatology	1/12, 1/4	Forward
C-3D	3-D	Climatology	1/12, 1/4	Forward
C-3DB	3-D, buoyant	Climatology	1/12, 1/4	Forward
C-BK	3-D	Climatology	1/12, 1/4	Backwards
R-SAR	3-D, buoyant, growth	Whole domain	1/4	Forward

eled on *Trichodesmium*), 1 zooplankton, and 2 detrital compartments of different sizes and remineralization rates. All of the living compartments have fixed N:P ratios, while the detrital compartments are allowed variable stoichiometry. Model structure is adapted from the work of Fennel et al. (2006), with addition of inorganic phosphorus, diazotrophy, and changes to phytoplankton light response after Hood et al. (2001) and Coles & Hood (2007). The Polar Science Center Hydrographic Climatology (Steele et al. 2001) is used for nutrient initial conditions and boundary relaxation. Model equations are described in the Supplement (www.int-res.com/articles/suppl/m599p001_supp.pdf). Normalized root mean square (RMS) error between model fields and SeaWiFS monthly chl *a* climatologies ranged from 0.009 to 0.016 (O'Reilly et al. 2000, SeaWiFS Project 2003). These residuals are slightly lower than those for sea surface temperature.

Sargassum model description

A *Sargassum* model runs within each Lagrangian particle, with each particle representing a super-individual aggregate of *Sargassum.* At each time step, *Sargassum* is advected by the particle model, and then growth and mortality are calculated based on ambient conditions at the particle location. This physiology model represents a functional group of pelagic *Sargassum* rather than either species specifically, so rates are selected from the range for both *S. fluitans* and *S. natans* during parameter optimization. *Sargassum* super-individuals within each Lagrangian particle are modeled with a macroalgal framework that includes light (I), temperature (T), and nutrient conditions (N) based on the biogeochemical model.

$$\frac{\mathrm{d}Sarg}{\mathrm{d}t} = Sarg \times f(I) \times f(T) \times f(N) \times \mu max_{\mathrm{S}} - m \times Sarg \quad (1)$$

Mortality (m) here is the aggregate effect of senescence and grazing, where μmax_{S} is *Sargassum* maximum growth rate and m is *Sargassum* mortality rate.

Because the Lagrangian approach allows for tracking the fate of discrete aggregations of *Sargassum,* modeled light availability accounts for the growth of epiflora and epifauna as a function of super-individual age:

$$f(I) = (1 - \mathrm{e}^{-I/I_{\mathrm{k}}}) \times f(age) \quad (2)$$

with an exponential decay in light response at increasing ages:

$$f(age) = \mathrm{e}^{-age/a_{\mathrm{ref}}} \quad (3)$$

where a_{ref} is the reference age for *Sargassum* light limitation due to colonization by epiflora and epifauna.

Nutrient uptake is modeled as a Monod function:

$$f(N) = \frac{N}{k_{Sarg} + N} \quad (4)$$

where N is the limiting nutrient (NO_3, NH_4, or DIP).

Growth experiments suggest little effect of temperature on *Sargassum* growth above 18°C (Carpenter & Cox 1974), with reduced growth below this temperature for both species (Hanisak & Samuel 1987). *S. fluitans* may experience low-temperature stress starting at 24°C (Hanisak & Samuel 1987), however observations of *Sargassum* below 18°C showed signs of distress and wilting (Winge 1923). For this reason, we implement a temperature dependence with a threshold for growth at 18°C.

$$f(T) = \begin{cases} 1, Temp \geq T_{\mathrm{ref}} \\ 0, Temp < T_{\mathrm{ref}} \end{cases} \quad (5)$$

The *Sargassum* model also includes pressure-induced sinking. Buoyancy of *Sargassum* floats is diminished at relatively shallow depths, and they are fully compromised by excursions to 120 m (Johnson & Richardson 1977, Woodcock 1993). Any *Sargassum* particle that descends below the maximum depth of float integrity (z_{max}) becomes too dense to recover and all biomass is lost via sinking.

We perform parameter optimization because several model parameters have few or no reported values in the literature for pelagic *Sargassum,* and because we are using a *Sargassum* functional group rather than explicitly modeling both species. A 3-way optimization tests 12 possible values for each parameter (1728 total parameter combinations) to select the parameter values that minimize error with satellite fields. Each model solution is compared with observations by binning both the satellite climatologies and model output onto an identical 2° grid and computing the RMS difference. This RMS error is averaged over the model domain monthly. The optimal parameter values, used in all subsequent simulations, are shown in Table 2. Note that the nutrient half saturation value is likely biased to be low because the biogeochemical model tends to have slightly low surface nutrient concentrations.

Particle model validation

HYCOM model fields have been widely utilized in studies of particle dispersal (Coles et al. 2013, Put-

Table 2. *Sargassum* physiology model parameters

Symbol	Parameter	Value	Unit	Literature range	Source
μmax_S	*Sargassum* maximum growth rate	0.1	d^{-1}	0.029–0.11	Lapointe (1986), Lapointe et al. (2014), Hanisak & Samuel (1987)
m	*Sargassum* mortality rate	0.05	d^{-1}	25–60% of gross productivity	Carpenter & Cox (1974), Lapointe (1995)
I_k	*Sargassum* growth-irradiance parameter	70	W m^{-2}	33–78	Hanisak & Samuel (1987), Lapointe (1995)
a_{ref}	Reference age for *Sargassum* light limitation	55	d	*	Thiel & Gutow (2005)
k_{SargN}	*Sargassum* nutrient uptake half saturation	0.012	mmol N m^{-3}	**	Lapointe (1986), Lapointe (1995), Carpenter & Cox (1974)
T_{ref}	Minimum temperature for *Sargassum* growth	18	°C	18–24	Carpenter & Cox (1974), Hanisak & Samuel (1987)
z_{max}	Maximum depth before *Sargassum* buoyancy is compromised	120	m	35–135	Johnson & Richardson (1977)

*No literature values are reported for this parameter. Initial estimates for parameter optimization were made based on maximum age of other rafting macroalgae and the growth rates of *Sargassum* epiphytes

**No direct measurements are reported for this parameter; however, see references for examples of growth and nutrient concentrations measured under varying environmental conditions

man & He 2013, Rypina et al. 2013, Stukel et al. 2014) and model validation studies have been published for the global domain (Chassignet et al. 2003, 2009). Here we concentrate on how well the model particles compare with the limited set of surface observational drifter data to ensure the surface currents relevant to *Sargassum* dispersal are captured reasonably, and to identify potential regions of divergence. Drifter observations for drogued drifters within the model domain region are obtained from the Global Drifter Program Drifter Data Assembly Center (Hansen & Poulain 1996). Model particles are launched to match initial drifter observations, with 7 particles initialized on the same day of the year and distributed within 3 km of each observed launch. These particles are tracked for 1 yr (Fig. 3).

After 2 mo, the distributions of observed drifters (Fig. 3a) and model particles (Fig. 3b) differ by less than 1% particle density in any given 2° × 2° bin. At this time scale, there is slightly higher retention of observed drifters in the Gulf of Mexico and near the Bahamas, but both model and observed drifters show the highest densities in the northwest region of the domain off of Georges Bank. Although the number of observed drifters with a full year of tracking data is low (n = 310), there is good agreement between the model and observations (Fig. 3c). The bulk of the drifters aggregate in the central gyre after 1 yr. Observed drifters show slightly greater spread, especially in the region northwest of the Gulf Stream, where eddy activity in the model may be resolution-limited. However, because model particles are removed when they go aground, particle density in the model tends to be very low near to the coastline, which explains some of the discrepancy.

RESULTS AND DISCUSSION

The role of advection

If *Sargassum* is initially evenly distributed throughout the Atlantic at low densities below satellite detection limits, as a result of winter mixing processes for example, seasonal variations in advection could potentially generate aggregations similar to the observed seasonal patterns. Lagrangian particle experiment R-ISO (Table 1) tests this hypothesis.

Randomly seeded, surface-restricted particles are launched every day for 1 yr over the whole domain (Fig. 4a). Transport of particles from the tropics through the Caribbean archipelago helps to maintain some particle density in the Gulf of Mexico at 2 mo

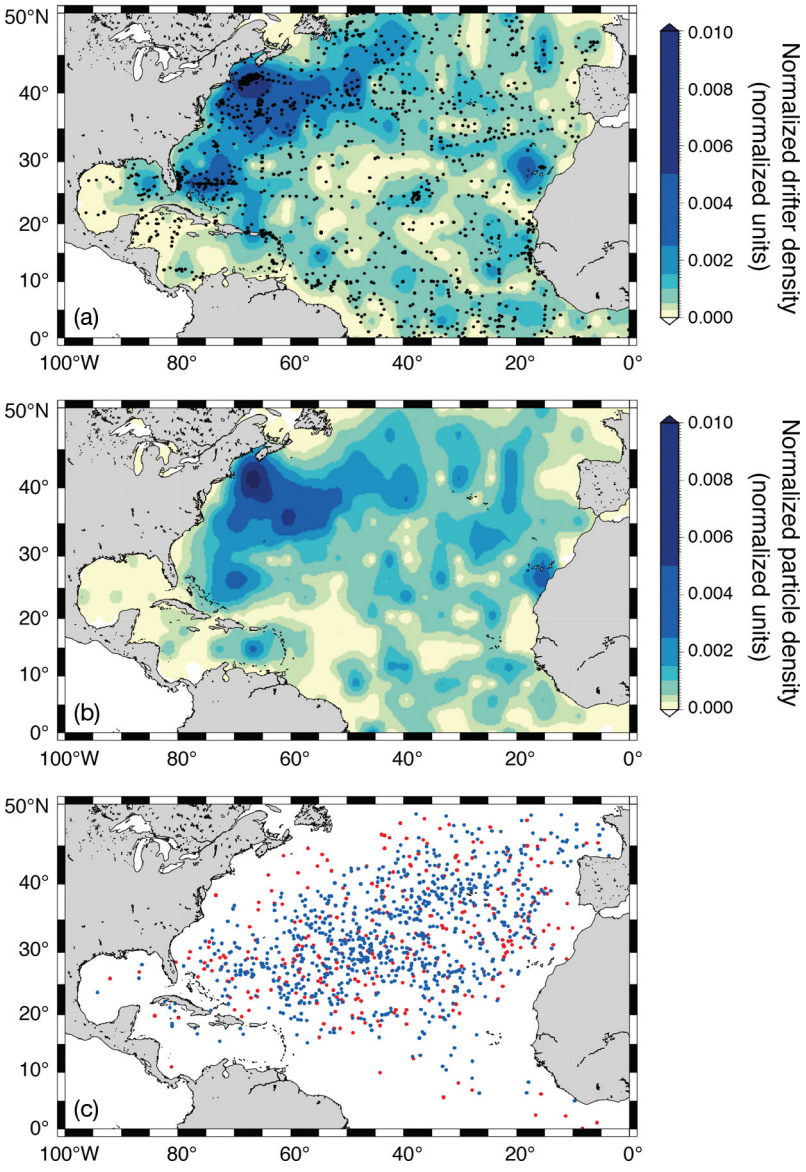

Fig. 3. Comparison of observed drifters and model particles. Density distributions for (a) observed, and (b) modelled drifters after 60 d transit time. Black points are model and drifter launch positions. (c) Observed (red) and modelled (blue) drifter locations after 1 yr transit time

time scales (Fig. 4b). After 6 mo (Fig. 4c), particle density is reduced by half in the Gulf of Mexico. Particle densities are also reduced at the northern and southern extents of the domain, due to loss of particles from the domain to the north, and to inflow of waters devoid of particles from the south. Particles are lost from the coast of Africa and the tropics due to upwelling and divergence in the Tropical Gyre and Guinea Dome (near 20° W, 15° N). After 1 yr, there is a strong tendency for particle aggregation in the North Atlantic Subtropical Gyre (Fig. 4d). At this time scale, particle densities in the central gyre have increased by an order of magnitude, while ecologically important regions such as the Caribbean and Gulf of Mexico are almost completely devoid of particles. The particle distribution resembles that of surface plastics in the region (Law et al. 2010) due to convergent Ekman flow, rather than the observed *Sargassum* distribution.

We subsequently examine each of the following assumptions: that *Sargassum* is highly buoyant and surface-restricted, that *Sargassum* exists at low densities throughout the domain, and that *Sargassum* behaves like a passive particle. The assumption that *Sargassum* is surface-restricted is tested first. *Sargassum* aggregations are frequently observed drifting subsurface. Small-scale, wind-driven features such as Langmuir cells can drive them as deep as 100 m (Johnson & Richardson 1977), and wind speeds as low as 4 m s^{-1} can result in subsurface *Sargassum* (Woodcock 1993). In experiment R-3D, the randomly initialized particles are neutrally buoyant 3-dimensional particles, and experiment R-3DB added positive buoyancy of 0.1 m s^{-1}. Both of these simulations resulted in particles aggregating in the central gyre at long time scales similarly to R-ISO (not shown). Particle density distributions for these 3 experiments converged after 6 mo, with pairwise FUV < 0.05 after 1 yr. At long time scales, particles initialized at the surface aggregate in the central gyre due to Ekman transport whether they are surface-restricted, neutrally buoyant, or slightly positively buoyant.

To test whether the *Sargassum* seasonal cycle is dependent on initial conditions, we initialize model particles based on the derived satellite climatologies. Particles are initialized daily in a randomly generated pattern within contours where MCI > 1% of maximum. Simulations with surface-restricted (C-ISO), neutrally buoyant (C-3D) and positively buoyant (C-3DB) particles initialized in accordance with monthly satellite climatologies of *Sargassum* all yield similar aggregated particle densities in the gyre at time scales of 6 mo or greater. Surface-constrained particles (Fig. 5) have slightly higher densities in the northern portion of the subtropical gyre

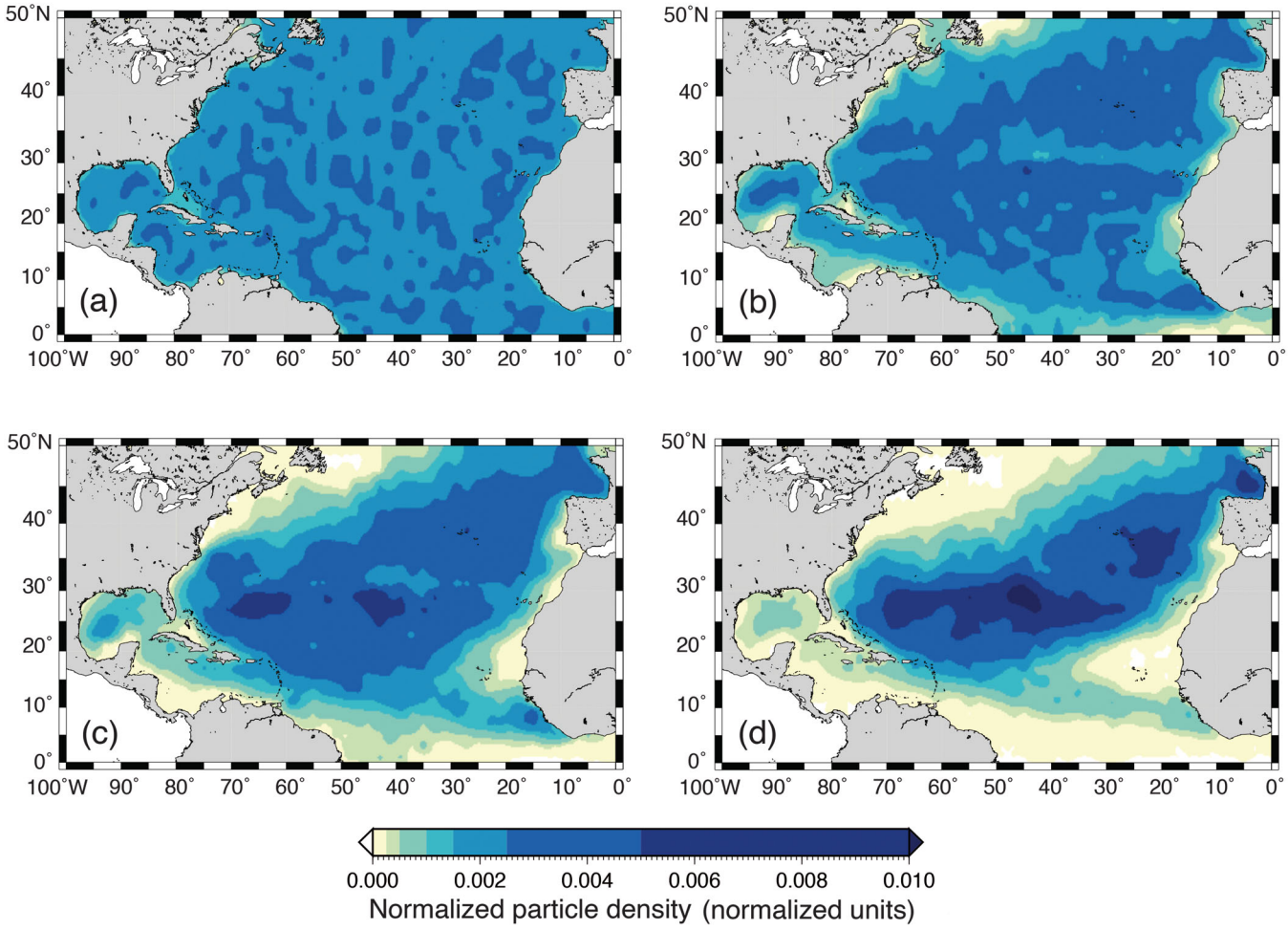

Fig. 4. Particle density distribution for randomly seeded surface particles. (a) Initial condition, and (b–d) distribution after (b) 60, (c) 180, and (d) 360 d particle transit time. The initial, randomly dispersed distribution ends up concentrated in the central gyre at time scales between 60 and 360 d

than 3-D positively buoyant particles (not shown) since there are some losses from the surface layers when the 3-D particles experience winter mixing. However, all 3 experiments result in the same pattern of aggregation in the gyre despite their observationally determined initial condition.

At shorter time scales, particles initialized in this way more closely match observations, and we examine monthly distributions to determine the degree of short-term advective control on *Sargassum*. We track model particles which originate within a given monthly observed distribution over a 2 mo period to determine what fraction remain within the satellite derived contours of *Sargassum* observations 2 mo later (e.g. Fig. 6b in September). Observed GDP drifters (Hansen & Poulain 1996) in the domain are also analyzed with an identical method (Fig. 6a).

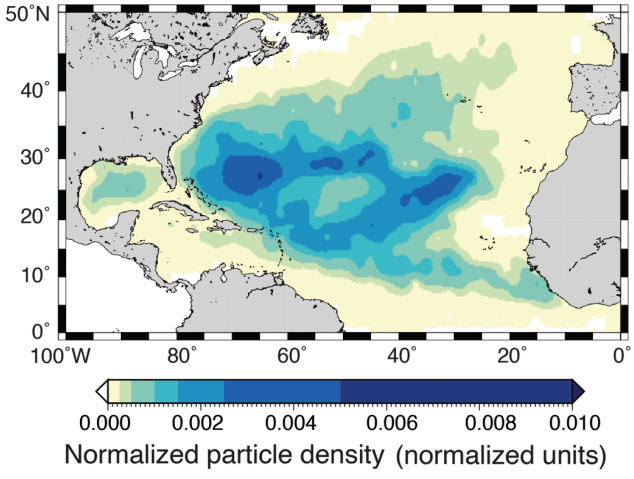

Fig. 5. Effects of particle motion. Surface-constrained particles initialized according to monthly climatologies of *Sargassum* biomass aggregate in the central gyre after 1 yr

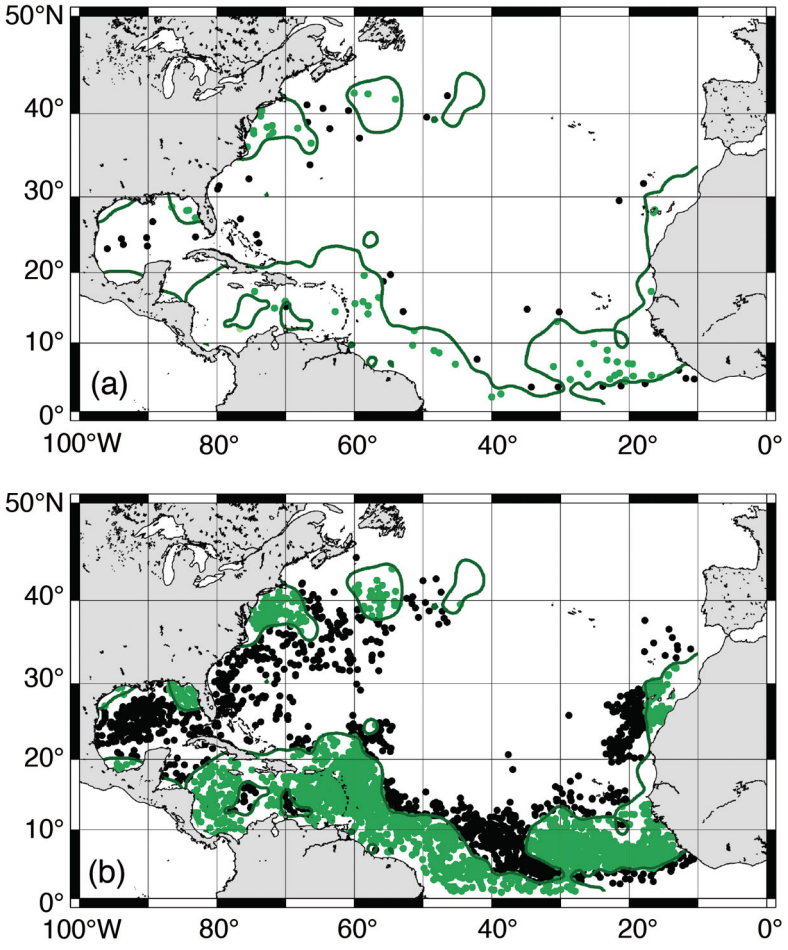

Fig. 6. Match in September between observed drifters, model floats, and satellite observations after 60 d transit time. Only (a) observed drifters and (b) model floats that originated in *Sargassum*-containing regions are shown. Contours are 1% of maximum MCI from *Sargassum* satellite climatology. Green points fall within the bounds of observations, black points represent mismatch

Match rate for particle location is calculated by counting particles within boundaries defined by a 1 km buffer around the 1% contour of MCI from the satellite climatology. This match rate is normalized to the total number of drifters or particles in the domain. The potential maximum match rate is expected to be below 100% due to discrepancies in comparing individual years to a climatology, limitations of model resolution, and small numbers of observed drifters.

The match rate is bimodal for both observed and modelled drifters (Fig. 7), with a peak in late winter and a stronger peak in late summer/early fall. Although the sample size for observed drifters is small (fewer than 10 drifters are present in *Sargassum*-dense areas in some mont hs), the overall pattern is consistent with our Lagrangian particles. These match rates are much higher and more strongly seasonally varying than the distributions for all observed drifters in the domain or for randomly distributed model particles (Fig. 7). Examining 3 mo and longer time intervals continues to show a distinct peak in match rate until time scales exceed 6 mo. Beyond that time period, the overall match is low and variable. After a full year, only 15% of the particles initialized in *Sargassum*-dense regions are still consistent with *Sargassum* observations. Thus, initial *Sargassum* distribution influences the final distribution for up to 6 mo.

The seasonality of the match rate indicates that processes other than advection are influencing the *Sargassum* distribution. Elevated match in the winter (months 2 to 4) is consistent with *Sargassum* experiencing lower temperatures and suppressed growth

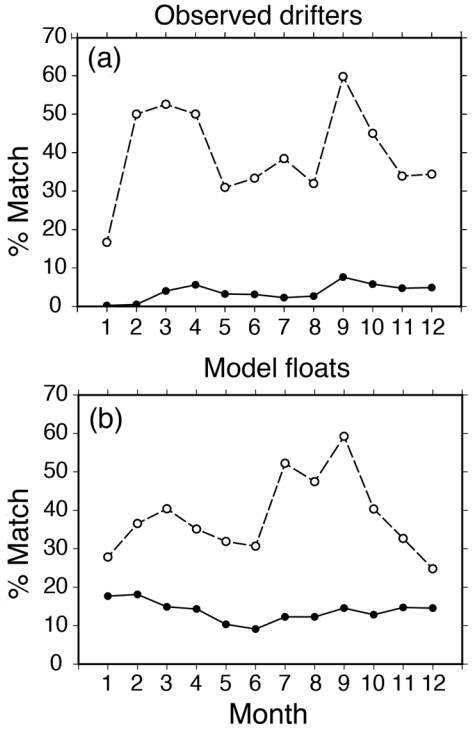

Fig. 7. Percent match rate with satellite observations of *Sargassum* for (a) observed drifters, and (b) modeled floats. Upper, dashed lines are drifters or floats that originate in regions where *Sargassum* is observed. Lower, solid lines include all observed drifters (a), and all randomly initialized floats (b). Both model and observations show a peak in % match in the fall, indicating high advective control on the *Sargassum* distribution at that time

(Hanisak & Samuel 1987), causing physical transport to explain more of the spatial distribution. A maximum match of 59% of model particles (Fig. 7b) occurs in the month of September, indicating another period where advection plays a large role in determining the *Sargassum* distribution. The subtropical water column is strongly stratified in September, leading to low nutrient conditions and reduced vertical mixing which make it more likely that surface transport rather than growth is controlling the *Sargassum* density. Periods of minimum match rate in December and June indicate times when *Sargassum* physiology may be more important in setting its distribution.

Gower & King (2011) proposed that the *Sargassum* seasonal cycle begins in the Gulf of Mexico in March-April with *Sargassum* growth advected out to the Atlantic, where it eventually senesces about a year later in the southern Sargasso Sea. To evaluate this hypothesis, we track buoyant, 3-D particles initialized in the Gulf of Mexico in experiment C-3DB, to quantify what fraction exit into the Atlantic within 1 yr, and whether there is a seasonal pattern. Connectivity between the Gulf of Mexico and the Sargasso Sea (Fig. 8) is high, with 29% of particles reaching the Atlantic within 1 yr. Particles are 5 times as likely to make this passage within 3 mo of launch as they are at longer time scales (Fig. 8a). The seasonal peak in particles crossing into the Atlantic in August (Fig. 8b) is a result of the large *Sargassum* biomass observed in the Gulf of Mexico in the spring and early summer exiting the region at this 3 mo time scale. However, with less than 1/3 of *Sargassum* exiting the Gulf within 1 yr, there must be robust growth of *Sargassum* after leaving the Gulf or additional seeding from other sources to match the densities seen in the northern Sargasso Sea in the fall.

However, the *Sargassum* originating in the Gulf of Mexico does not contribute to high density of *Sargassum* in the tropics. Trajectories of randomly seeded surface particles initialized in the Gulf of Mexico (Fig. 9a) and the Caribbean (Fig. 9b) remain exclusively north of 10° N after 1 yr. *Sargassum* originating in the tropics (Fig. 9c) does reach the Caribbean and Gulf of Mexico at this time scale. Even accounting for transit times longer than 1 yr, *Sargassum* from the Gulf of Mexico does not reach the tropics, since the convergent North Atlantic Subtropical Gyre is essentially a dead end (Fig. 9d). Connectivity analysis shows that over 92% of particles launched in the Caribbean in the spring (that did not run aground) are advected into the subtropical gyre after 1 yr. For the western and eastern Gulf of Mexico 54% and 81% of particles, respectively, are found in the subtropical

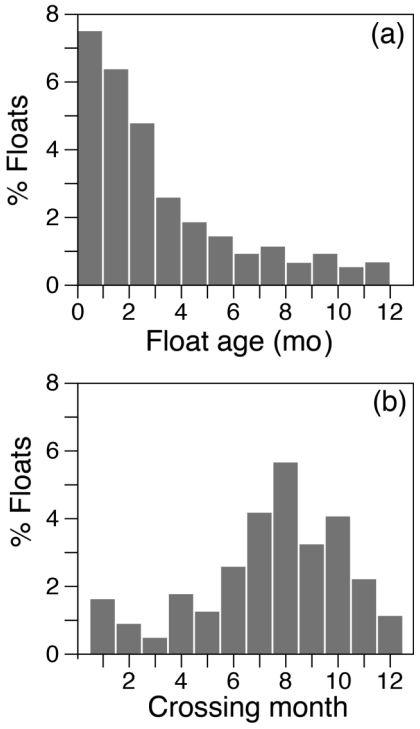

Fig. 8. Floats exiting the Gulf of Mexico. (a) Age and (b) month at exit, defined as crossing 81° W, of model floats initialized randomly in the Gulf of Mexico over 1 model yr

gyre after 1 yr, while the rest remain within the Gulf. None of these regions export particles to the tropics at any time scale from 30 to 360 d. This suggests that a southern or eastern source of *Sargassum* is necessary to account for biomass in the tropics and Caribbean. This is supported by the connectivity between the Western Tropical Atlantic, which exports particles to the tropics (77%), but also to the Gulf of Mexico (5%) and Caribbean (8%), with the remainder entering the subtropical gyre.

To better understand the connectivity between regions and to potentially highlight source regions of *Sargassum* we conducted an experiment in which we ran particles backwards in time (C-BK). Particles are initialized using the *Sargassum* monthly climatology for each month, and run with a negative time step for 60 d (Fig. 10). The central and eastern subtropical gyre is largely devoid of particles, confirming the pattern seen in Fig. 9d where particles tend to remain confined to that region. The highest densities of particles are found along the coast of Brazil and along the equator, suggesting again the potential for a southern source for *Sargassum* in the tropics. These results are consistent with recent evidence of links between the equatorial population and beachings

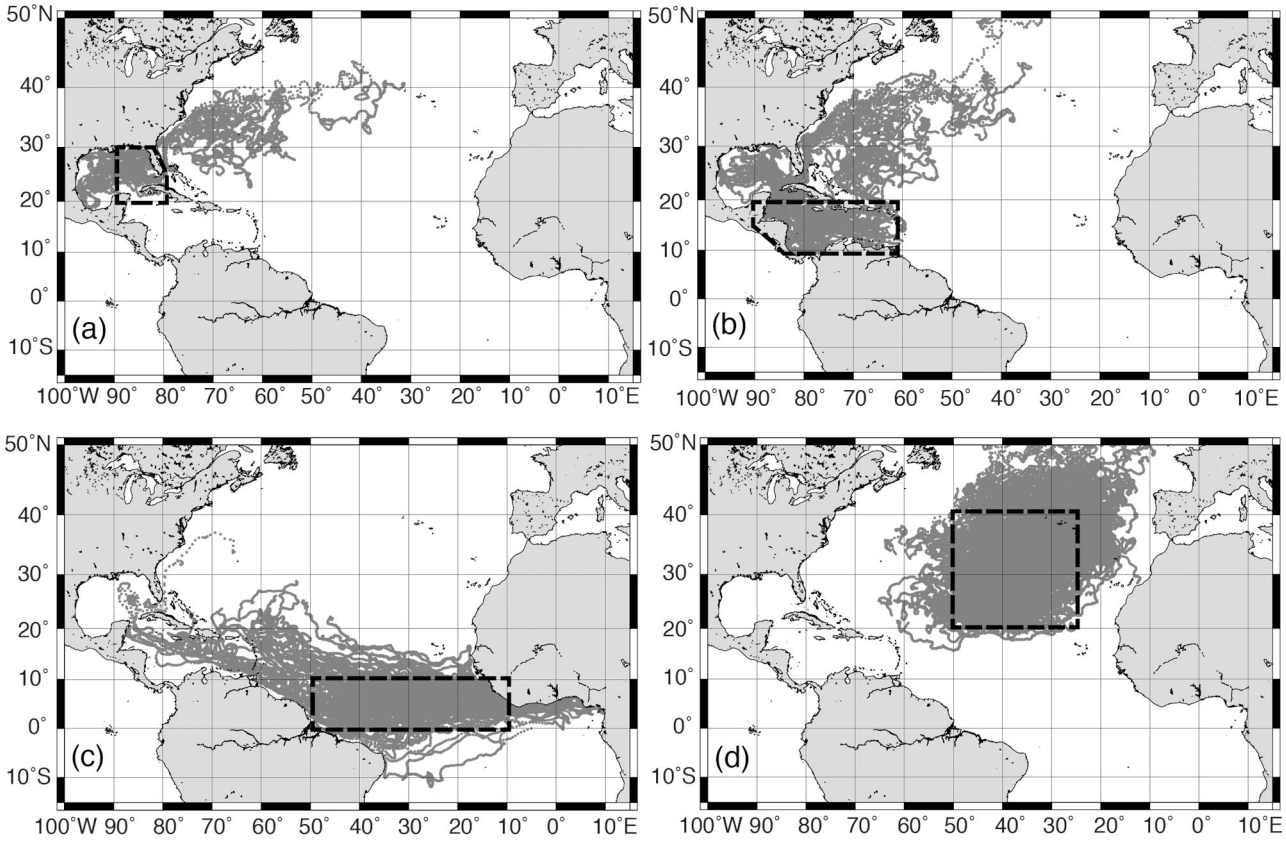

Fig. 9. A subsample of trajectories over 1 yr for particles launched in (a) the eastern Gulf of Mexico, (b) the Caribbean Sea, (c) the central tropics, and (d) the subtropical gyre. Dashed boxes indicate particle launch region

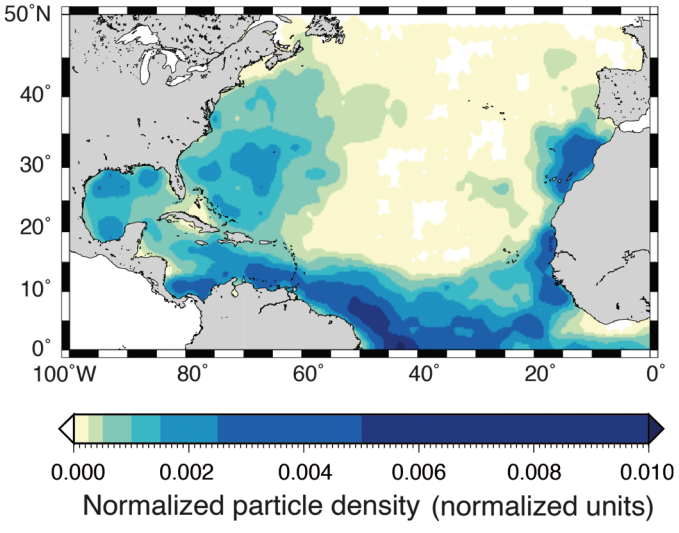

Fig. 10. Particle density for 3-D particles initialized from *Sargassum* monthly satellite climatologies and run backwards in time. This distribution integrates the seasonal cycle by including all particles of age −60 d

of *Sargassum* in the Caribbean (Franks et al. 2016). Of particular interest, our results suggest a pathway for connectivity between the putative large equatorial population (Gower et al. 2013) and the Caribbean and Gulf of Mexico. Even though relatively few particles follow this pathway, over 60% of the particles in the Gulf and Caribbean track back to this hypothetical tropical population.

The time scales associated with the travel of these particles indicate that equatorial *Sargassum* observed between December and February could be contributing to the peak in *Sargassum* biomass in the Gulf of Mexico between May and July. Match percent between particles run backwards for 2 mo and observed *Sargassum* distributions showed that 50% of particles track back to regions that do not match observations. This suggests that low densities of *Sargassum*, invisible to satellites, could contribute to blooms over much of the Atlantic as they are advected into regions with favorable growth conditions.

Sargassum model

To determine the role *Sargassum* biology plays in driving its seasonal distribution, we apply the *Sargassum* super-individual model to each particle in a 1/4° HYCOM simulation which is coupled with a biogeochemistry model (simulation R-SAR). We conduct a sensitivity analysis to understand which parameters have the largest impact on the *Sargassum* model. Single parameter model sensitivity is evaluated for all *Sargassum* model parameters (Table 2), focused on a range bounded by ± 10% of reported values, where available. Mortality, nutrient uptake half saturation, and reference age for light limitation are the parameters with the greatest impact on model solutions. The combined impact of grazing and mortality is about a 5% loss d^{-1}, and *Sargassum* older than 55 d begins to experience notable light limitation from growth of epiflora and epifauna or from loss of buoyancy.

For *Sargassum* growth experiments, particles are initialized daily across the model domain for 6 yr. Nitrogen, phosphorus, light and temperature are sampled at each daily particle location and input into the *Sargassum* physiology model. Particle density maps are similar to the results from 1/12° physics-only simulations indicating that reducing the horizontal model resolution did not significantly alter the particle dispersion characteristics at the spatiotemporal scale of this analysis (Fig. 11a). The match between model (Fig. 11b) and observations (Fig. 1d) is greatly improved by including *Sargassum* biomass from the *Sargassum* physiology model in the particle density calculation (Fig. 11c). Biomass is higher in and near regions of high observed *Sargassum* density, and dramatically reduced in the central gyre where low nutrient conditions are unfavorable for growth. Growth rates approached their maximum of 0.1 d^{-1} most frequently in the tropics in winter, suggesting a stronger role for nutrients than for light and temperature in controlling *Sargassum* growth. The percent match between model and observations (Fig. 12a) is higher when *Sargassum* physiology is included than for any other simulation. The match rate is also consistently high throughout the year, implying that *Sargassum* growth and mortality are large contributors to the observed distribution even during periods when advective control is also high.

Because observed *Sargassum* distribution is patchy, we estimate the best possible model fit to observations by comparing the observed interannual variability to the monthly climatology. We use the RMS error between satellite derived *Sargassum* biomass for 10 individual years and the climatology to characterize observed variability (Fig. 12b). The

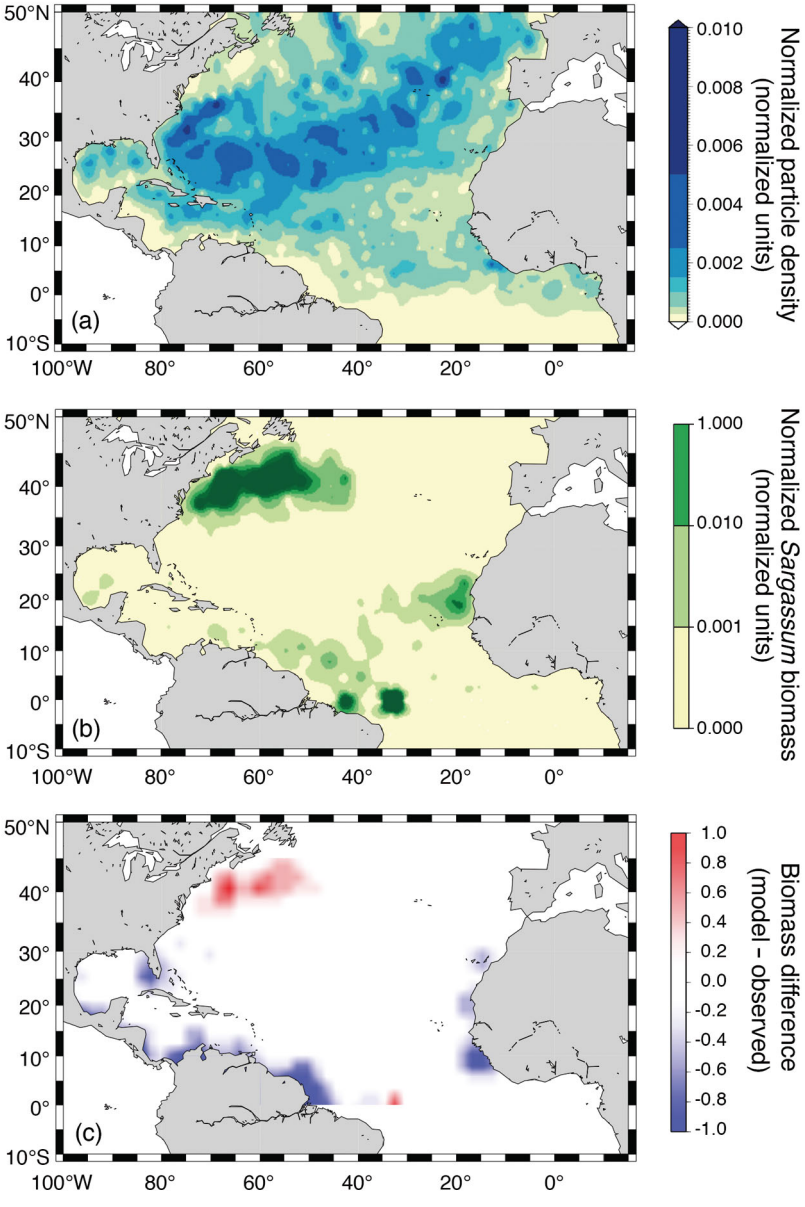

Fig. 11. (a) Particle density in November without *Sargassum* growth. (b) Normalized *Sargassum* model biomass. (c) Difference between *Sargassum* model and observed normalized biomass. Model *Sargassum* biomass is consistent with observations, in contrast to the high abiotic particle densities in the central gyre

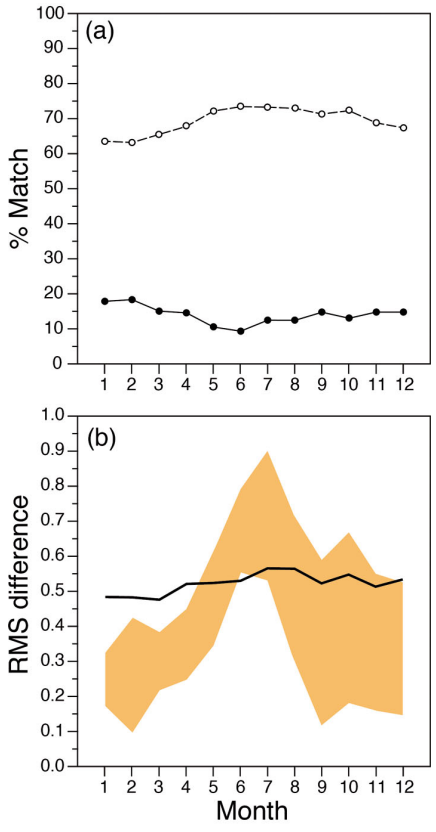

Fig. 12. Model performance. (a) Percent match between randomly initialized particles with (dashed line) and without (solid line) accounting for *Sargassum* growth. (b) Root mean square (RMS) difference between model and satellite climatologies for the model (black line) and individual years of satellite data (shaded region indicates mean ± SD). Match with observations is high, consistent throughout the year, and generally within the bounds of observed biomass variability

mean RMS difference between the observations and climatology is 0.44, while the RMS difference between the model and climatology is 0.50. Variability in biomass in the tropics in the spring and summer accounted for the highest differences between individual years of observations and the climatologies. For the model, RMS differences peaked slightly later in the summer and early fall when *Sargassum* biomass is starting to diminish in the tropics. On an annual basis, the model biomass falls within the range of variability of the satellite observations.

Sargassum seed populations

This model still underestimates *Sargassum* biomass in the tropics over much of the year even when nutrient, temperature, and light conditions are favorable. Biomass is overestimated elsewhere. Tropical *Sargassum* has high growth rates in the model, but is advected away too quickly to allow accumulation of biomass. One scenario that accounts for this missing *Sargassum* is import from outside our model domain. Observations of pelagic *Sargassum* off the coast of Africa are relatively recent in the literature (Oyesiku & Egunyomi 2011, Gower & et al. 2013), but evidence from local fishing communities suggests it has been present over at least several decades, although not at current densities (Ackah-Baidoo 2013). A modest export of *Sargassum* from a region such as the Gulf of Guinea, combined with favorable growth conditions, could be contributing to the high biomass across the tropical Atlantic (Franks et al. 2016).

We assess the potential that export from one or several sub-regions of the Atlantic sustains the seasonal distribution of *Sargassum* in a series of model seeding experiments. Particles are initialized daily in 17 sub-regions with average area of 1.32×10^6 km^2 in the Sargasso Sea and along the coastlines on both sides of the basin, at the same density as the whole-domain experiments for 6 yr. Notably, seeding in any of the individual sub-regions yields better match with observed *Sargassum* distributions than initializing across the entire domain (Fig. 13, gray bars), again suggesting that although *Sargassum* has the potential to be dispersed throughout the Atlantic, these dispersed fragments do not appear to be driving the seasonal cycle. The highest match between model and observations is obtained by seeding particles in the western Gulf of Mexico, west of 90° W (RMS difference = 0.36), the southwestern tropical Atlantic between 5° S to 10° N and 40° W to 60° W (RMS difference = 0.35), or in both of these regions simultaneously (RMS difference = 0.34). A closer examination within individual sub-regions shows that while the basin-wide average agreement with observations is similar when seeding in either the southwestern tropics or the western Gulf of Mexico, only the experiment that seeded in both simultaneously reproduces the seasonal pattern in those locations (Fig. 12a), but still underrepresents peak *Sargassum* biomass, especially in the Sargasso Sea.

Another possible driver for seasonal changes in *Sargassum* biomass is vegetative reproduction. As pelagic *Sargassum* and related species break, new growth is primarily initiated from the residual fragments at apical meristems (Tsukidate 1984, Hanisak & Samuel 1987). We expand the model to include vegetative propagation by tracking when each *Sargassum* particle dies, and resetting its biomass to a small initial condition instead, simulating a small fragment of the *Sargassum* mat breaking off at that

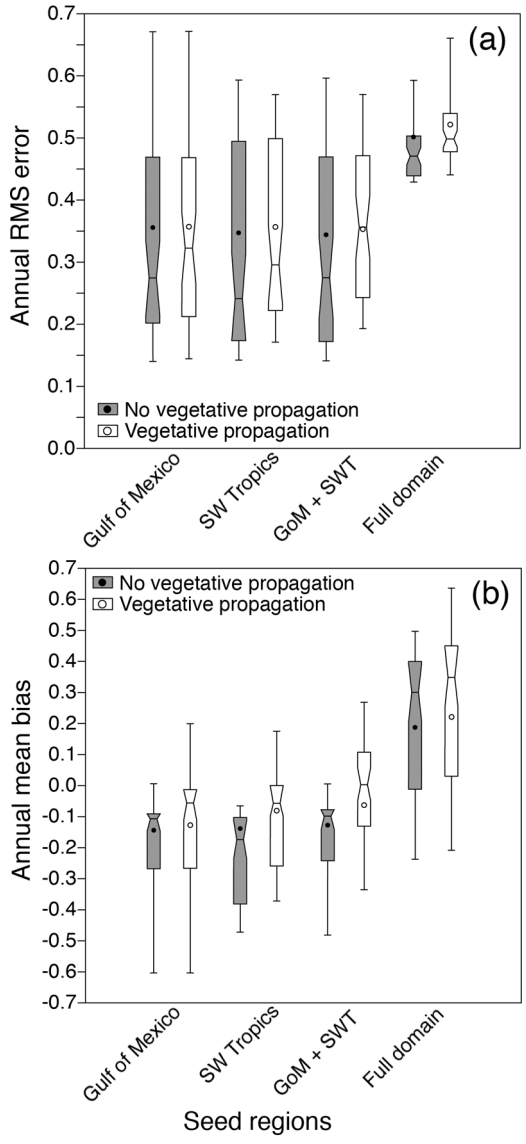

Fig. 13. (a) Root mean square (RMS) difference and (b) mean bias between model and observations for seeding and vegetative propagation experiments. Box-and-whiskers are aggregate results from analysis within individual subregions. Boxes indicate median and interquartile ranges and whiskers delineate full ranges. Circles are the mean bias calculated over the full model domain. Seeding in the 2 subregions reduces error and mean bias, while vegetative propagation further reduces mean bias

location to start a new organism. Since rafting macroalgae can have expected lifetimes on the order of months (Thiel & Gutow 2005), we apply this propagation mode only to *Sargassum* particles over 1 mo old. This avoids over-representation of biomass in regions with high mortality due to seasonal temperature changes or severe nutrient limitation. We apply vegetative propagation only to particles where the *Sargassum* has died because fragmentation and growth at other times is assumed to be aggregated with the other biomass in a given particle.

We repeat the 6-yr, full-domain model experiments with vegetative propagation enabled. Simulations with and without this reproductive strategy added have comparable RMS differences of 0.52 and 0.50 respectively, when compared with the monthly satellite climatologies. However, without vegetative propagation the model has a negative bias in mean relative *Sargassum* biomass of −10 to −40% of the maximum in the western Atlantic and Gulf of Mexico, while the bias with vegetative propagation is much smaller and more centered about the mean (−7% to +1.5%) (Fig. 13, white bars). Vegetative propagation also yields increased match with observations in seeding experiments with sources of *Sargassum* in the Gulf of Mexico and southwestern

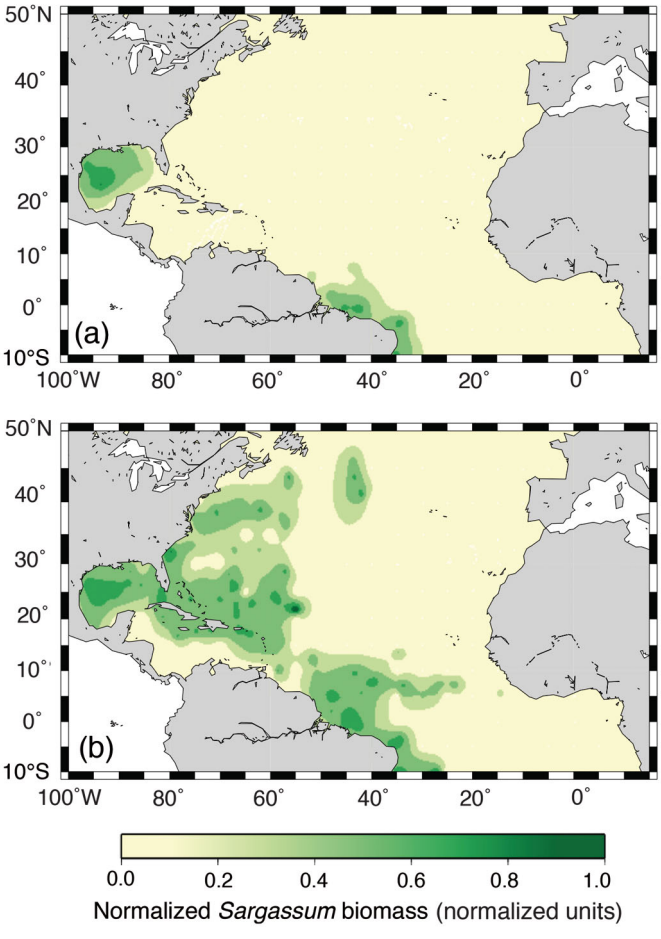

Fig. 14. Seeding and vegetative propagation experiments. (a) Seeding in the Gulf of Mexico and southwestern tropics reproduces local patterns but underrepresents *Sargassum* biomass elsewhere in the domain. (b) With vegetative propagation, *Sargassum* biomass in the Sargasso Sea can result from advection and growth of nonlocal sources

tropics, while allowing increased accumulation of biomass in the Sargasso Sea (Fig. 14). Without vegetative propagation, local patterns are reproduced but the basin-wide distribution is unrealistic without seeding across the domain because of the difference between the mortality rate and the time scale of advection (Fig. 14a). The addition of vegetative propagation allows biomass accumulation in the Caribbean and Sargasso Sea from nonlocal sources. Thus, the additive effects of vegetative propagation and localized sources of new *Sargassum* appear to be key in accurately reproducing the *Sargassum* seasonal cycle.

CONCLUSIONS

At short time scales of 2 mo or less, advection alone can be responsible for a 60% match between model particles and *Sargassum* observations, indicating that advection is a central element determining *Sargassum* distributions in the Atlantic. However, at longer time scales, particles, whether surface, neutrally buoyant, or positively buoyant, aggregate in the subtropical gyre. This aggregation occurs regardless of whether particles are initialized throughout the Atlantic or only in regions with observed *Sargassum*. Thus, advection is not sufficient to maintain the seasonal pattern of *Sargassum* biomass across multiple years. This highlights the significance of mortality, growth, and reseeding from putative source regions in maintaining *Sargassum*'s seasonal distribution.

Results of seeding experiments with the *Sargassum* growth model highlight that the western Gulf of Mexico and the western tropics, especially south of the equator, appear to have a strong role in generating the seasonal cycle. These regions are associated with 2 of the largest rivers discharging into the Atlantic, the Mississippi and the Amazon. Nutrient loading may enhance *Sargassum* growth locally in these 2 regions, however even under the globally high discharge of the Amazon, inorganic nitrogen falls below detection limits about 200 km from the river mouth (Weber et al. 2017). Neritic waters near the coastline have also been linked with higher growth rates of *Sargassum* than in the central Sargasso Sea in observations (Lapointe et al. 2014). In this model, that growth is what allows for high *Sargassum* biomass even in regions that would otherwise have low accumulation due to the circulation.

It is also noteworthy that due to the circulation patterns in the Atlantic, we are unable to reproduce the seasonal biomass pattern without continuous seeding in both key regions, as there are no purely advective pathways for *Sargassum* from the Gulf of Mexico to reach the tropics at biologically relevant time scales. The backwards-timestep particles and connectivity analysis presented here also support the hypothesis that *Sargassum* in the tropics has a southern source. Different morphological forms of *S. natans* appear to be dominant in the Sargasso Sea versus the Western Tropics (Schell et al. 2015), which is consistent with this two-source hypothesis. Additional observational studies would be helpful in determining if *Sargassum* biomass is present in the proposed seed regions year-round, and whether the genetic diversity of *Sargassum fluitans* and *Sargassum natans* supports this hypothesis.

The Western Tropical Atlantic source region is of particular interest due to its potential role in fueling beaching events in the Caribbean. Reverse-time modeling and observed drifters suggest that *Sargassum* from recent beaching events in the eastern Caribbean and Brazil may have originated in the equatorial region (Franks et al. 2011, 2016). Biomass in the tropics is highest in the summer, during the period of eastward retroflection of the Amazon plume in the North Equatorial Counter Current. However, there is also year-round connectivity between the Amazon plume and the Caribbean, with water discharged from the Amazon in the spring having the highest probability of reaching the Caribbean (Coles et al. 2013). The connectivity analysis in this study is consistent with the results of Coles et al. (2013), and also shows that the connectivity from the tropics to the Caribbean is higher than any other potential source in the Atlantic. This provides a mechanism for a direct link between the elevated *Sargassum* biomass in the tropics in recent years and the increased reports of *Sargassum* beaching in the Caribbean.

We propose a scenario where the *Sargassum* seasonal cycle begins in the spring with growth in the tropics and the western Gulf of Mexico, in agreement with analysis of the satellite observations alone (Gower & King 2011). Biomass from the tropics gets advected through the Caribbean to the Gulf, supplementing local growth there into the summer. This model highlights how connectivity between the Gulf of Mexico and the Sargasso Sea, in conjunction with direct inputs from the population in the tropics, fuels growth in the Sargasso Sea in summer and early fall. At this point temperature and light constrain growth at the northern extent of *Sargassum*'s range, and advection works to aggregate biomass toward the Sargasso Sea, where much of the biomass is exported in the late winter. Regions of high *Sargassum* mortal-

ity in this model are consistent with observations of *Sargassum* on the sea floor (Schoener & Rowe 1970) and warrant further study as a possible locally important source of carbon export. This enhanced understanding of the drivers of the *Sargassum* seasonal cycle should help inform management of fisheries dependent on *Sargassum* habitat, and forecasting of costly *Sargassum* wash-up events in the Caribbean and Gulf of Mexico.

Acknowledgements. The authors thank Lou Codispoti, Judy O'Neil, and Zulema Garraffo for insightful discussions regarding this work. We also thank the 3 anonymous reviewers whose comments greatly improved the manuscript. This research is part of the Blue Waters sustained-petascale computing project, which is supported by the National Science Foundation (awards OCI-0725070 and ACI-1238993) and the state of Illinois. Blue Waters is a joint effort of the University of Illinois at Urbana-Champaign and its National Center for Supercomputing Applications. This work was also funded in part by a University of Maryland Center for Environmental Science Horn Point Laboratory Bay and Rivers Fellowship. M.B. led the modeling effort in collaboration with V.C. and R.H. Satellite data and interpretation was provided by J.G. This manuscript is UMCES contribution #5501

LITERATURE CITED

Ackah-Baidoo A (2013) Fishing in troubled waters: oil production, seaweed and community-level grievances in the western region of Ghana. Community Dev J 48:406–420

Beron-Vera FJ, Olascoaga MJ, Haller G, Farazmand M, Triñanes J, Wang Y (2015) Dissipative inertial transport patterns near coherent Lagrangian eddies in the ocean. Chaos 25:087412

Butler JN, Stoner AW (1984) Pelagic *Sargassum*: has its biomass changed in the last 50 years? Deep-Sea Res A 31: 1259–1264

Butler JN, Morris BF, Cadwallader J, Stoner AW (1983) Studies of *Sargassum* and the *Sargassum* community. Bermuda Biol Stn Spec Publ 22

Carpenter EJ, Cox JL (1974) Production of pelagic *Sargassum* and a blue-green epiphyte in the western Sargasso Sea. Limnol Oceanogr 19:429–436

Carr A, Meylan AB (1980) Evidence of passive migration of green turtle hatchlings in *Sargassum.* Copeia 1980: 366–368

Chassignet EP, Smith LT, Halliwell GR (2003) North Atlantic simulations with the HYbrid Coordinate Ocean Model (HYCOM): impact of the vertical coordinate choice, reference pressure, and thermobaricity. J Phys Oceanogr 33:2504–2526

Chassignet E, Hurlburt H, Metzger EJ, Smedstad O and others (2009) US GODAE: Global ocean prediction with the HYbrid Coordinate Ocean Model (HYCOM). Oceanography (Wash DC) 22:64–75

Coles VJ, Hood RR (2007) Modeling the impact of iron and phosphorus limitations on nitrogen fixation in the Atlantic Ocean. Biogeosciences 4:455–479

Coles VJ, Brooks MT, Hopkins J, Stukel MR, Yager PL, Hood RR (2013) The pathways and properties of the Amazon River plume in the tropical North Atlantic Ocean. J Geophys Res Oceans 118:6894–6913

Cummings JA (2005) Operational multivariate ocean data assimilation. Q J R Meteorol Soc 131:3583–3604

Cummings JA, Smedstad OM (2013) Variational data assimilation for the global ocean. In: Park SK, Xu L (eds) Data assimilation for atmospheric, oceanic and hydrologic applications (Vol II). Springer, Berlin, p 303–343

Deacon GER (1942) The Sargasso Sea. Geogr J 99:16–28

Dickson HN (1894) Recent contributions to oceanography. Geogr J 3:302–310

Fennel K, Wilkin J, Levin J, Moisan J, O'Reilly J, Haidvogel D (2006) Nitrogen cycling in the Middle Atlantic Bight: Results from a three-dimensional model and implications for the North Atlantic nitrogen budget. Global Biogeochem Cycles 20:GB3007

Franks JS, Johnson DR, Ko DS, Rubio GS, Hendon JR, Lay M (2011) Unprecedented influx of pelagic *Sargassum* along Caribbean island coastlines during summer 2011. Proc Gulf Caribb Fish Inst 64:6–8

Franks JS, Johnson DR, Ko DS (2016) Pelagic *Sargassum* in the tropical North Atlantic. Gulf Caribb Res 27:SC6-11

Garraffo ZD, Mariano AJ, Griffa A, Veneziani C, Chassignet EP (2001) Lagrangian data in a high resolution numerical simulation of the North Atlantic. I: Comparison with in-situ drifter data. J Mar Syst 29:157–176

Gower JFR, Hu C, Borstad G, King S (2006) Ocean color satellites show extensive lines of floating *Sargassum* in the Gulf of Mexico. IEEE Trans Geosci Remote Sens 44: 3619–3625

Gower JFR, King SA (2011) Distribution of floating *Sargassum* in the Gulf of Mexico and the Atlantic Ocean mapped using MERIS. Int J Remote Sens 32:1917–1929

Gower JFR, Young E, King S (2013) Satellite images suggest a new *Sargassum* source region in 2011. Remote Sens Lett 4:764–773

Halliwell GR, Weisberg RH, Mayer DA (2003) A synthetic float analysis of upper-limb meridional overturning circulation interior ocean pathways in the tropical/subtropical Atlantic. In: Goni GJ, Malanotte-Rizzoli P (eds) Interhemispheric water exchange in the Atlantic Ocean. Elsevier Oceanogr Ser 68. Elsevier, Amsterdam p 93–136

Hanisak MD, Samuel MA (1987) Growth rates in culture of several species of *Sargassum* from Florida, USA. Hydrobiologia 151–152:399–404

Hansen DV, Poulain PM (1996) Quality control and interpolations of WOCE-TOGA drifter data. J Atmos Ocean Technol 13:900–909

Hoffmayer ER, Franks JS, Comyns BH, Hendon JR, Waller RS (2005) Larval and juvenile fishes associated with pelagic *Sargassum* in the Northcentral Gulf of Mexico. Proc Gulf Caribb Fish Inst 56:259–269

Hood RR, Bates NR, Capone DG, Olson DB (2001) Modeling the effect of nitrogen fixation on carbon and nitrogen fluxes at BATS. Deep-Sea Res II 48:1609–1648

Hu C, Feng L, Hardy RF, Hochberg EJ (2015) Spectral and spatial requirements of remote measurements of pelagic *Sargassum* macroalgae. Remote Sens Environ 167: 229–246

Huffard CL, von Thun S, Sherman AD, Sealey K, Smith KL (2014) Pelagic *Sargassum* community change over a 40−year period: temporal and spatial variability. Mar Biol 161:2735–2751

Johnson DL, Richardson PL (1977) On the wind-induced sinking of *Sargassum.* J Exp Mar Biol Ecol 28:255–267

Laffoley Dd'A, Roe HSJ, Angel MV, Ardron J and others (2011) The protection and management of the Sargasso Sea: The golden floating rainforest of the Atlantic Ocean. Summary science and supporting evidence case. Sargasso Sea Alliance, IUCN, Washington, DC

Lapointe BE (1986) Phosphorus-limited photosynthesis and growth of *Sargassum natans* and *Sargassum fluitans* (Phaeophyceae) in the western North Atlantic. Deep-Sea Res A 33:391–399

Lapointe BE (1995) A comparison of nutrient-limited productivity in *Sargassum natans* from neritic vs. oceanic waters of the western North Atlantic Ocean. Limnol Oceanogr 40:625–633

Lapointe BE, West LE, Sutton TT, Hu C (2014) Ryther revisited: Nutrient excretions by fishes enhance productivity of pelagic *Sargassum* in the western North Atlantic Ocean. J Exp Mar Biol Ecol 458:46–56

Law KL, Morét-Ferguson S, Maximenko NA, Proskurowski G, Peacock EE, Hafner J, Reddy CM (2010) Plastic accumulation in the North Atlantic subtropical gyre. Science 329:1185–1188

North EW, Gallego A, Petitgas P (eds) (2009) Manual of recommended practices for modelling physical-biological interactions during fish early life. ICES Coop Res Rep 295

O'Reilly JE, Maritorena S, O'Brien MC, Siegel DA and others (2000) SeaWiFS postlaunch calibration and validation analyses, part 3. SeaWiFS Postlaunch Tech Rep Ser 11

Oyesiku OO, Egunyomi A (2011) Identification and chemical studies of pelagic masses of *Sargassum natans* (Linnaeus) Gaillon and *S. fluitans* (Borgessen) Borgesen (brown algae), found offshore in Ondo State, Nigeria. Afr J Biotechnol 13:1188–1193

Parr AE (1939) Quantitative observations on the pelagic *Sargassum* vegetation of the western North Atlantic. Bull Bingham Oceanogr Coll Yale Univ 6:1–94

Putman NF, He R (2013) Tracking the long-distance dispersal of marine organisms: sensitivity to ocean model resolution. J R Soc Interface 10:20120979

Rast M, Bezy JL, Bruzzi S (1999) The ESA Medium Resolution Imaging Spectrometer MERIS: a review of the instrument and its mission. Int J Remote Sens 20:1681–1702

Rypina II, Jayne SR, Yoshida S, Macdonald AM, Douglass E, Buesseler K (2013) Short-term dispersal of Fukushima-derived radionuclides off Japan: modeling efforts and model-data intercomparison. Biogeosciences 10:4973–4990

Schell JM, Goodwin DS, Siuda ANS (2015) Recent *Sargassum* inundation events in the Caribbean: shipboard observations reveal dominance of a previously rare form. Oceanography (Wash DC) 28:8–10

Schoener A, Rowe GT (1970) Pelagic *Sargassum* and its presence among the deep-sea benthos. Deep-Sea Res, Oceanogr Abstr Oceanogr Bibliogr Sect 17:923–925 doi.org/10.1016/0011-7471(70)90010-0

SeaWiFS Project (2003) SeaWiFS global monthly mapped 9 km chlorophyll *a*. Ver. 1. https://podaac.jpl.nasa.gov/dataset/SeaWiFS_L3_CHLA_Monthly_9km_R

Simons RD, Siegel DA, Brown KS (2013) Model sensitivity and robustness in the estimation of larval transport: a study of particle tracking parameters. J Mar Syst 119–120:19–29

Sissini MN, de Barros Barreto MBB, Széchy MTMd, de Lucena MB and others (2017) The floating *Sargassum* (Phaeophyceae) of the South Atlantic Ocean — likely scenarios. Phycologia 56:321–328

Siuda ANS (2011) Summary of Sea Education Association long-term Sargasso sea surface net data. Sargasso Sea Alliance Science Rep Ser 10

Smetacek V, Zingone A (2013) Green and golden seaweed tides on the rise. Nature 504:84–88

Steele M, Morley R, Ermold W (2001) PHC: A global ocean hydrography with a high-quality Arctic Ocean. J Clim 14:2079–2087

Stoner AW (1983) Pelagic *Sargassum*: evidence for a major decrease in biomass. Deep-Sea Res A 30:469–474

Stukel MR, Coles VJ, Brooks MT, Hood RR (2014) Top-down, bottom-up and physical controls on diatom-diazotroph assemblage growth in the Amazon River plume. Biogeosciences 11:3259–3278

Széchy MTMd, Guedes PM, Baeta-Neves MH, Oliveira EN (2012) Verification of *Sargassum natans* (Linnaeus) Gaillon (Heterokontophyta: Phaeophyceae) from the Sargasso Sea off the coast of Brazil, western Atlantic Ocean. Check List 8:638–641

Thiel M, Gutow L (2005) The ecology of rafting in the marine environment. I. The floating substrata. Oceanogr Mar Biol Annu Rev 42:181–264

Tsukidate J (1984) Studies on the regenerative ability of the brown algae, *Sargassum muticum* (Yendo) Fensholt and *Sargassum tortile* C. Agardh. Hydrobiologia 116-117: 393–397

Uppala SM, Kållberg PW, Simmons AJ, Andrae U and others (2005) The ERA-40 re-analysis. Q J R Meteorol Soc 131: 2961–3012

Wang M, Hu C (2016) Mapping and quantifying *Sargassum* distribution and coverage in the Central West Atlantic using MODIS observations. Remote Sens Environ 183: 350–367

Weber SC, Carpenter EJ, Coles VJ, Yager PL, Goes J, Montoya JP (2017) Amazon River influence on nitrogen fixation and export production in the western tropical North Atlantic. Limnol Oceanogr 62:618–631

Webster RK, Linton T (2013) Development and implementation of *Sargassum* Early Advisory System (SEAS). Shore Beach 81:1–6

Winge Ø (1923) The Sargasso Sea, its boundaries and vegetation. Rep Danish Oceanogr Exped 1908–1910 to Mediterr Adjac Seas 3:1–34

Witherington B, Hirama S, Hardy R (2012) Young sea turtles of the pelagic *Sargassum*-dominated drift community: habitat use, population density, and threats. Mar Ecol Prog Ser 463:1–22

Woodcock AH (1993) Winds subsurface pelagic *Sargassum* and Langmuir circulations. J Exp Mar Biol Ecol 170: 117–125

Zhong Y, Bracco A, Villareal TA (2012) Pattern formation at the ocean surface: *Sargassum* distribution and the role of the eddy field. Limnol Oceanogr Fluids Environ 2:12–27

Editorial responsibility: Claire Paris, Miami, Florida, USA

Submitted: November 22, 2017; Accepted: May 18, 2018
Proofs received from author(s): June 30, 2018